Case studies in computer-aided molecular design (CAMD) of low- and medium-grade waste-heat recovery ORC systems

L.M.T. van Kleef, O.A. Oyewunmi, A.A. Harraz, A.J. Haslam and C.N. Markides*

Clean Energy Processes (CEP) Laboratory, Department of Chemical Engineering,
Imperial College London, South Kensington Campus, London, SW7 2AZ, UK.
** Corresponding author. Email: c.markides@imperial.ac.uk; Tel. +44 (0)20 759 41601*

Abstract:

Organic Rankine cycle (ORC) engines are suitable for the conversion of low-grade heat into useful power. While numerous substances are available as ORC working-fluid candidates, computer-aided molecular design (CAMD) techniques allow the rigorous selection of an optimal working fluid during system optimisation. The aim of this present study is to extend an existing CAMD-ORC framework [1,2] by incorporating, in addition to thermodynamic performance objectives, economic objectives when determining the optimal system design, while maintaining the facility of selecting optimal working fluids. The SAFT-γ Mie equation of state is used to predict the thermodynamic properties of the working fluids (here, hydrocarbons) that are relevant to the systems' economic appraisals and critical/transport properties are estimated using empirical group-contribution methods. System investment costs are estimated with equipment cost correlations for the key system components, and the stochastic NSGA-II solver is used for system optimisation. From a set of NLP optimisations, it is concluded that the optimal molecular size of the working fluid is linked to the heat-source temperature. The optimal specific investment cost (SIC) values were £10,120/kW and £4,040/kW when using heat-source inlet temperatures of 150 °C and 250 °C (representative of low- and medium-grade heat) respectively, and the corresponding optimal working fluids were propane, 2-butane and 2-heptene.

Keywords:

computer-aided molecular design (CAMD); low-grade heat; organic Rankine cycle (ORC); statistical associating fluid theory (SAFT); thermo-economic optimization; waste-heat recovery

1. Introduction

Converting low-grade heat into electrical power has the potential to significantly increase energy efficiency of industries, thereby reducing primary fuel use and CO_2 emissions [3]. This conversion can be performed more efficiently with organic Rankine cycle (ORC) engines, when compared to a regular Rankine cycle engine that deploys steam [4]. Currently, ORC systems are already being implemented on a kW to MW scale for the conversion of waste heat, solar heat and heat from biomass combustion. The determination of the optimal ORC engine specifications has received significant attention in the literature, and computer-aided optimisation techniques offer the opportunity to apply effective and systematic searches. This provides a more all-encompassing systems design method than traditional methods that do not incorporate economic considerations in the optimisation objective or those that involve a pre-selection of working fluids.

The development of computer-aided molecular design (CAMD) methods has allowed the systematic selection of a chemical design during process/system optimisation, thereby omitting the subjective preselection of conventional compounds [5,6]. In this approach, molecules are described as combinations of smaller structural groups. Theoretically, any arbitrary molecule can be described as a collection of such groups, given that all relevant groups are incorporated in the decision space.

Multiple authors have included CAMD techniques in the optimisation of ORC systems (including those with mixtures as working fluids), while using (semi-)empirical group-contribution (GC) methods and equations of state (EoS) [7-11]. An inherent disadvantage of an empirical EoS is a

potentially low degree of accuracy, especially when conditions or substances are assessed for which no experiments have been performed. Furthermore, the prediction of second order derivative quantities, such as the specific heat capacity, tends to be relatively inaccurate [12]. A modern family of equations of state, based on the statistical associating fluid theory (SAFT), does not have this limitation. Using SAFT, it is possible to predict thermodynamic properties, even if they are out of the experimental data range [13]. Several formulations of SAFT have been developed, such as PC-SAFT [14], SAFT-VR Mie [15] and SAFT-γ Mie [13]. PC-SAFT and SAFT-γ Mie are compatible with GC approaches. Dufal *et al.* show that SAFT-γ Mie is capable of accurately predicting vapour-liquid equilibrium data of pure components and mixtures of several hydrocarbons [16], as well as second derivative properties. A detailed description of SAFT-γ Mie is presented in Ref. [13].

Several authors have applied SAFT-based equations of state in CAMD optimization studies of ORC systems. Lampe *et al.* developed a two-stage CAMD-ORC framework with the PC-SAFT EoS, which they called 'continuous-molecular targeting CAMD' (CoMT-CAMD) [17]. Both the maximum net power output and a minimum temperature at the heat source outlet were used as optimisation objectives. The authors did not incorporate an economic evaluation in the optimisation framework. White *et al.* and Oyewunmi *et al.* applied a CAMD-ORC optimisation approach for basic ORC systems, using the SAFT-VR Mie and SAFT-γ Mie as equations of state for both pure and mixture working fluids [1,18-20]. These authors performed thermodynamic optimisations, maximising the power generation for waste-heat recovery applications.

The works listed above focussed solely on thermodynamic performance of ORC systems. However, a technical optimisation is only a first step in the actual implementation of ORC systems [21]. Both performance and economic feasibility should be considered to determine an optimal system [18]. The economic feasibility of new energy technologies is mainly determined by the investment costs, and the estimation of capital cost has received a lot of attention in this context [22]. Only a few authors have combined CAMD techniques and economic assessment of ORC systems. Schilling *et al.* devised a multi-objective CAMD-ORC optimisation framework, where both the total investment costs and the rate of power generation were used as objectives [23]. The effect of different heat source temperatures is not investigated here, and no analysis is provided regarding the optimal working conditions within the cycle. Recently, White *et al.* proposed a framework to assess both thermodynamic and economic performance of a waste heat recovery ORC system [2], however, economic objectives were not considered during the initial optimisation procedure.

The integration of a SAFT-based EoS within a CAMD-ORC optimisation framework has the potential to identify novel working fluids that lead to enhanced performance. Only a few studies consider the investment costs in parallel with the thermodynamic performance of the optimised systems. The aim of this study is to extend the existing CAMD-ORC framework developed by White *et al*. with detailed equipment sizing models. The developed framework allows for simultaneous system optimisation and working fluid selection, while taking into account both thermodynamic performance and system costs. Optimisations are performed with the stochastic NSGA-II algorithm. Furthermore, the effect of the heat source temperature and the choice of objective function on the optimal working fluid and system design will be considered.

2. ORC system model

The framework consists of a thermodynamic cycle, heat exchanger models and investment cost correlations. The molecular groups considered are $–CH_3$, $–CH_2–$, $>CH–$, $>C<$, $=CH_2$ and $=CH–$, where –, = and > denote single, double and two single bonds respectively. The working fluid is defined by assigning integer values to each molecular group, representing the quantity of each group present in the working fluid molecules. Next to the integer variables describing the working fluid, the six continuous decision variables that are varied during the optimisation are the condensing temperature (T_1), the reduced pressure in the evaporator (P_r), the internal temperature difference in the evaporator (ΔT_x), the normalised degree of superheating (z) and the working fluid velocities in the evaporator (v_{ev}) and the condenser (v_{co}). These variables are described in the following section.

2.1. Thermodynamic cycle

A typical temperature-specific entropy (*T*-*s*) diagram of a subcritical non-recuperated ORC is shown in Fig. 1. At each of the states depicted in Fig. 1, the thermodynamic state variables such as entropy (s), heat capacity (c_p), enthalpy (h) and density (ρ) are estimated using the SAFT-γ Mie EoS. The thermodynamic model used in this study is based on the work by White *et al*. [1], with the model validated by comparison with another CAMD-ORC optimisation study performed by Schilling *et al.* [17]. For completeness, a brief overview of the thermodynamic model is provided.

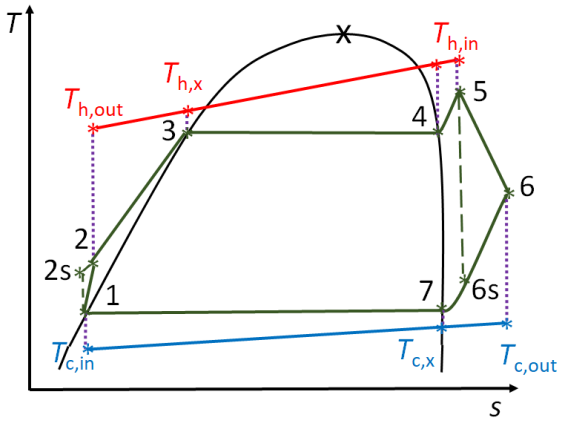

Fig. 1. T-s diagram of a basic subcritical non-recuperated ORC.

It is assumed that the working fluid is a saturated liquid at State 1, thus its thermodynamic state is determined by the condensation temperature, T_1. Irreversibilities during the pumping and expansion processes are accounted for by defining isentropic pump and expander efficiencies ($\eta_{is,pump}$, $\eta_{is,tur}$). In the evaporator, the decision variable ΔT_x is calculated as in Eq. 1. The amount of superheating, and thus the outlet temperature T_5, is determined by a normalized variable z, as shown in Eq. 2:

$$\Delta T_x = T_{h,x} - T_3, \quad (1) \qquad T_5 = T_4 + z * (T_{h,in} - T_4). \quad (2)$$

Pressure drops are neglected in the heat exchangers, however, to overcome the pressure drops in the cycle, more pump work is required. Therefore, the heat exchanger design is not merely related to the costs of the system but directly influences engine performance. To account for the pressure drop in the evaporator (ΔP_{ev}), the pump delivers additional work and increase the pressure from P_1 to $P_2 + \Delta P_{ev}$ (instead of just from P_1 to P_2, as assumed in the thermodynamic cycle model). Similarly, to account for the pressure drop in the condenser (ΔP_{co}), the working fluid can only expand from P_5 to $P_6 + \Delta P_{co}$ (instead of from P_5 to P_6). This ensures that the working fluid can overcome the ΔP_{co} and leaves the condenser at a pressure of P_1. The rate of electrical power consumption by the pump ($\dot{W}_{pump}$) and rate of power generation by the turbine ($\dot{W}_{tur}$) are computed as the enthalpy difference over the respective processes, while considering pressures corrected for pressure drops:

$$\dot{W}_{pump} = \dot{m}_{wf} * (h_{pump} - h_1), \quad (3) \qquad \dot{W}_{tur} = \dot{m}_{wf} * (h_5 - h_{tur}), \quad (4)$$

where h_{pump} and h_{tur} denote the specific enthalpies of the working fluid at the outlets of the pump and turbine, corrected for pressure drops in the heat exchangers and $\dot{m}_{wf}$ is the working-fluid mass flowrate. Finally, the rate of net power generation ($\dot{W}_n$) is determined as:

$$\dot{W}_n = \dot{W}_{tur} - \dot{W}_{pump}. \quad (5)$$

2.2. Group-contribution methods and validation

The inclusion of molecular groups to define working fluids requires the use of group-contribution (GC) methods to determine molecular and transport properties such as P_{cr} and T_{cr}, μ, λ and σ, which are not obtainable from the current SAFT-γ Mie capabilities. These properties influence heat transfer, and are required to estimate heat transfer coefficients (α), thus distinct correlations are employed for the liquid and vapour phases (subscript L and V, respectively). The critical properties (P_{cr}, T_{cr} and V_{cr})

and the accentric factor (ω) are evaluated from Joback and Reid correlations [24] and Ambrose and Walton [25], respectively. Liquid viscosity (μ_L) is estimated from Joback and Reid correlations and Sastri and Rao (branched alkanes) [26], while vapour viscosity (μ_V) is from Reichenberg [27]. Thermal conductivities (λ_L and λ_V) are estimated from Sastri and Rao [28] and Chung [29,30] respectively, while surface tension (σ) is estimated from Sastri and Rao [31] for saturated liquids.

The use of the GC methods in ORC frameworks was validated in earlier work [1,32] by comparing predicted property values with reference data from REFPROP [33] for of a variety of hydrocarbons; reasonable accuracy was reported for the estimation of liquid and vapour μ and λ at low temperatures. For further validation, a comparison is made between the heat transfer areas (A_s) and specific investment cost (SIC) values as determined with GC methods or REFPROP data [32]. This is done for optimised systems with *n*-butane, isohexane and 1-propene with heat source temperatures ($T_{h,in}$) of 150 °C, 250 °C and 350 °C, respectively. Underestimation of the SIC between 0.7% and 4.3% are reported. Compared to the inaccuracy that is introduced by application of correlations for determining the costs (>±30%), this is a relatively small deviation. Furthermore, the GC methods allow the assessment of working fluids for which no data is available, thereby validating their use in an ORC system context.

2.3. Heat exchanger sizing

The evaporator and condenser are modelled as double-pipe tubular heat exchangers, with the working fluid flowing in the inner tube and the heat source or sink flowing through the annulus counter-currently. This type of heat exchanger is suitable for small to medium-scale applications and of relatively low capital costs due to simple design [34]. Furthermore, the temperature profiles achieved in these heat exchangers are representative of the profiles assumed in the thermodynamic model.

The decision variables related to the heat exchangers are the liquid velocities (v) of the working fluid, *i.e.*, v_{ev} at the inlet of the preheating section in the evaporator, and v_{co} at the outlet of the condensing section of the condenser. Based on these velocities, the mass flow rates and properties of the fluids, the diameters of the inner and outer pipes of the entire heat exchanger are obtained. The inner tube is assumed to be made of carbon steel with a thermal conductivity (k) of 60 W/(m K) and a thickness of 3.68 mm, which are typical values for double-pipe heat exchangers at moderate pressures [34].

The following well-known equations are used to size the heat exchangers:

$$\dot{Q} = A_s * U * \Delta T_{lm}, \qquad (6) \qquad \frac{1}{U} = \frac{1}{\alpha_{inner}} + \frac{D_{outer}}{D_{inner}} * \frac{1}{\alpha_{outer}} + \frac{D_{outer}}{2k} * \ln\left(\frac{D_{outer}}{D_{inner}}\right), \qquad (7)$$

where $\dot{Q}$ denotes the heat flux, U the overall heat transfer coefficient, ΔT_{lm} the logarithmic temperature difference between the streams, α the convective heat transfer coefficient, D the diameter and the subscripts 'inner' and 'outer' the inner and outer surfaces of the pipe, respectively. Depending on the phase of the working fluid, different correlations for α are used to determine U.

For all the single-phase streams, α is determined by the Dittus-Boelter correlation. For the two-phase evaporating and condensing sections, multiple two-phase correlations for α_{inner} are used. For the evaporating section, the asymptotic correlations by Chen, Dobson *et al.*, Steiner and Taborek, and Liu and Winterton [35-37] are employed. In every subsection, the heat transfer area (A_s) is calculated using the four distinct correlations for α_{inner}, and an average A_s is obtained for a subsection. In the condensing section of the condenser, a similar approach is used to calculate an average A_s for a subsection; correlations by Shah, Chaddock and Chato, and Boyko and Kruzhilin [38-40] are used.

The single-phase frictional pressure drop per unit length is calculated by:

$$\left(\frac{dP}{dx}\right)_f = -\frac{4f_0}{D_{inner}} * \left(\frac{\rho v^2}{2}\right), \qquad (8) \qquad f_0 = 0.046 * Re^{-0.2}, \qquad (9)$$

where subscript f denotes frictional, f_0 is the friction factor and *Re* the Reynolds number. The two-phase frictional pressure drop is calculated using the correlations proposed by Friedel [41]. By multiplying the required length of each subsection with the differential pressure drop, ΔP_f for the two-phase sections is obtained. The acceleration pressure drop (ΔP_a) during the complete phase change can be calculated by:

$$\Delta P_a = G^2 * \left(\frac{1}{\rho_{out}} - \frac{1}{\rho_{in}}\right), \qquad (10)$$

where ρ_{in} and ρ_{out} are the working fluid densities at the heat exchanger inlet/outlet, and G the mass flux.

2.4. Capital cost estimation

A common indicator used for preliminary economic assessment of ORC systems is the specific investment costs (SIC). This metric represents the total investment costs (TIC) of the system per kilowatt of net electrical power generated. Correlations from Turton *et al.* [42] and Seider *et al.* [43] are used to estimate the 'base bare module costs' ($C^0_{BM,i}$) of major equipment units. The 'bare module costs' ($C_{BM,i}$) are derived by accounting for the operating pressure and materials of construction, with an expected accuracy of ±30% [21]. To account for inflation since the development of these correlations, the 'chemical engineering plant cost index' (CEPCI) values are used. The costs are converted to 2017 values using a $CEPCI_{2017}$ of 556.8. Finally, a contingency factor of 18% is applied to account for inaccuracies introduced by using correlations for equipment costs and pressure factors, and a contractor fee factor [44].

2.5. Optimisation procedure

The optimizations are carried out using a MATLAB implementation of the stochastic 'non-dominating genetic algorithm II' (NSGA-II) solver which can solve both single or multiple objective(s) problem. An important aspect of such stochastic solvers are the parameters of the solver; those used in this study for different optimisation problems are presented in Table 1.

Table 1. Algorithm parameters for NSGA-II optimisation as used in this study.

Parameter	NLP	MINLP	Multi-objective
Maximum generations	60	150	200
Population size	150	400	500
Mutation fraction	0.3	0.6	0.7
Cross-over fraction	0.7	0.4	0.3
Mutation scale	0.5	0.5	0.5
Shrink factor	0.25	0.25	0.25
Cross-over ratio	1.5	1.5	1.5

The optimisation problem is formulated in the general structure presented below:

$$\min_{\boldsymbol{x},\boldsymbol{z}} \ \mathbf{f}(\boldsymbol{x},\boldsymbol{z}), \qquad (11)$$

$$\text{s.t.} \quad \mathbf{h}(\boldsymbol{x},\boldsymbol{z}) = 0,\ \mathbf{g}(\boldsymbol{x},\boldsymbol{z}) \leq 0,\ \boldsymbol{x} \in \left[\mathbf{x^{lo}}, \mathbf{x^{up}}\right] \subseteq \mathbb{R}^n,\ \boldsymbol{z} \in \left[\mathbf{z^{lo}}, \mathbf{z^{up}}\right] \subseteq \mathbb{N}^m.$$

Here, $\boldsymbol{x}$ is the set of n continuous system variables, representing continuous decision variables in the process model, and $\boldsymbol{z}$ is the set of m integer variables describing the quantity of each molecular group in the working fluid. Further, **f** is the vector of objective functions: the SIC, or the TIC, or the net power output ($\dot{W}_n$). The set of equalities **h** contains all equations related to the thermodynamic cycle, the GC methods, heat exchanger sizing and costing methodology as well as the well-known octet rule, which is used as molecular feasibility constraint [45]:

$$\sum_k n_k * (2 - v_k) - 2 = 0. \qquad (12)$$

Here, n_k denotes the integer amount of molecular group k present in the molecule, and v_k denotes the valency of molecular group k. The value of v_k represents the number of bonds a molecular group type must undergo to obtain eight electrons in the valence shell of the carbon atom. This ensures no bonds remain unused within a molecule.

3. Case studies and discussion of results

To analyse the results obtained by the framework and investigate how different system specifications influence the SIC, three waste-heat recovery case studies are investigated, similar to case studies

studied in Refs. [1,2]. The expander is assumed to be a single-stage radial turbine, as these have shown to be suitable for both medium to large-scale systems, as well as applications with low heat source temperatures [1]. For simplicity, specific turbine design characteristics such as the expansion ratio, rotor inlet blade velocity and rotor inlet Mach number are not considered in these case studies. Also, special material or seal requirements due to the working fluid nature are not taken into account here. These properties influence the suitability, efficiency and price of the turbine, and should be considered in future work. Further, it is assumed that an intermediate closed fluid-circuit connects the ORC engine to the heat source, since this decreases system sensitivity to changing heat source conditions and most commercial system employ such circuits [46]. The heat transfer fluid is assumed to be Therminol 66 in both investigated cases, supplied at 150 °C and 250 °C, of which accurate property predicting correlations have been determined. The heat sink is cooling water, entering the condenser at 15 °C. Both $\eta_{is,pump}$ and $\eta_{is,tur}$ are assumed to be 0.7. The remaining specifications are listed in Table 2.

Table 2. Waste-heat recovery case study specifications for the heat source and sink.

	T_{in} [°C]	$\dot{m}$ [kg/s]	c_p [J/kgK]	v [m/s]
Heat source (h)	150, 250	2.1	2,000	2
Heat sink (c)	15	5	4,200	1.5

A set of NLP optimisations is performed for the three case studies specified in Table 2, with the objective of minimising the SIC. The working fluid is chosen *a priori*, from four common hydrocarbon families: *n*-alkanes, isoalkanes, 1-alkenes and 2-alkenes, by varying the number of –CH_2– groups in the working fluid molecule. The general molecular formula of each hydrocarbon family is presented in Table 3. The remaining decision variables are T_1, P_r, z, ΔT_x, v_{ev} and v_{co}.

Table 3. The four common hydrocarbon families and their constituent molecular groups.

S/N	Hydrocarbon family	General formula	Molecular groups
I	*n*-alkanes	$H_3C–(CH_2)_n–CH_3$	$–CH_3$ and $–CH_2–$
II	isoalkanes	$(H_3C)_2–CH–(CH_2)_n–CH_3$	$–CH_3$, $–CH_2–$ and $>CH–$
III	1-alkenes	$H_3C–(CH_2)_n–CH=CH_2$	$–CH_3$, $–CH_2–$, $=CH–$ and $=CH_2$
IV	2-alkenes	$H_3C–(CH_2)_n–CH=CH–CH_3$	$–CH_3$, $–CH_2–$ and $=CH–$

3.1. Optimal ORC system power output and SIC from NLP optimisations

The results of minimising the specific investment costs (SIC) for each heat source and hydrocarbon family are presented in Fig. 4. Here, the SIC and corresponding $\dot{W}_n$, are plotted against the number of carbon atoms that are present in the working fluid. As can be seen in Fig. 2 (TOP), a substantial increase in $\dot{W}_n$ is observed with increasing $T_{h,in}$. The highest $\dot{W}_n$ values are 27.7 kW and 94.3 kW, in order of ascending $T_{h,in}$. From Fig. 2 (BOTTOM), it follows that, for each hydrocarbon family, the molecular size of the optimal working fluid (leading to the lowest SIC) increases with $T_{h,in}$. More specifically, the optimal molecular sizes are C_3/C_4 for $T_{h,in}$ = 150 °C and C_4/C_5 for $T_{h,in}$ = 250 °C. Thus, light working fluids are favoured for the low-temperature heat source, while working fluids of increasing molecular weight are chosen at higher temperatures. The best performing systems have propane and 2-butene as working fluids in increasing order of $T_{h,in}$. The corresponding SIC values are £10,120/kW and £4,040/kW. Thus, a decrease of the SIC values is observed as the heat-source temperature (and consequently the system size) increases.

In White *et al.* [1], optimisations on similar case studies were carried out, but with the objective of maximising $\dot{W}_n$. While an increase in $\dot{W}_n$ with $T_{h,in}$ was also reported, the $\dot{W}_n$ values reported are, on average, 37% higher than the values in Fig. 2 (TOP). This is not surprising as the objective in White *et al.* [1] was to maximise the $\dot{W}_n$, and the effect of pressure drops on the performance was not

accounted for. The working fluids that resulted in the maximum $\dot{W}_n$ were propane and 2-pentene, for the 150 °C and 250 °C heat sources, respectively [1], while the highest $\dot{W}_n$ values reported in Fig. 2 (TOP) are achieved with *n*-butane and 2-pentene (at 150 °C and 250 °C). Thus, using the SIC as objective function leads to a reduction in $\dot{W}_n$ (in comparison with maximising $\dot{W}_n$), and in the low temperature case, a different working fluid that achieves the highest $\dot{W}_n$.

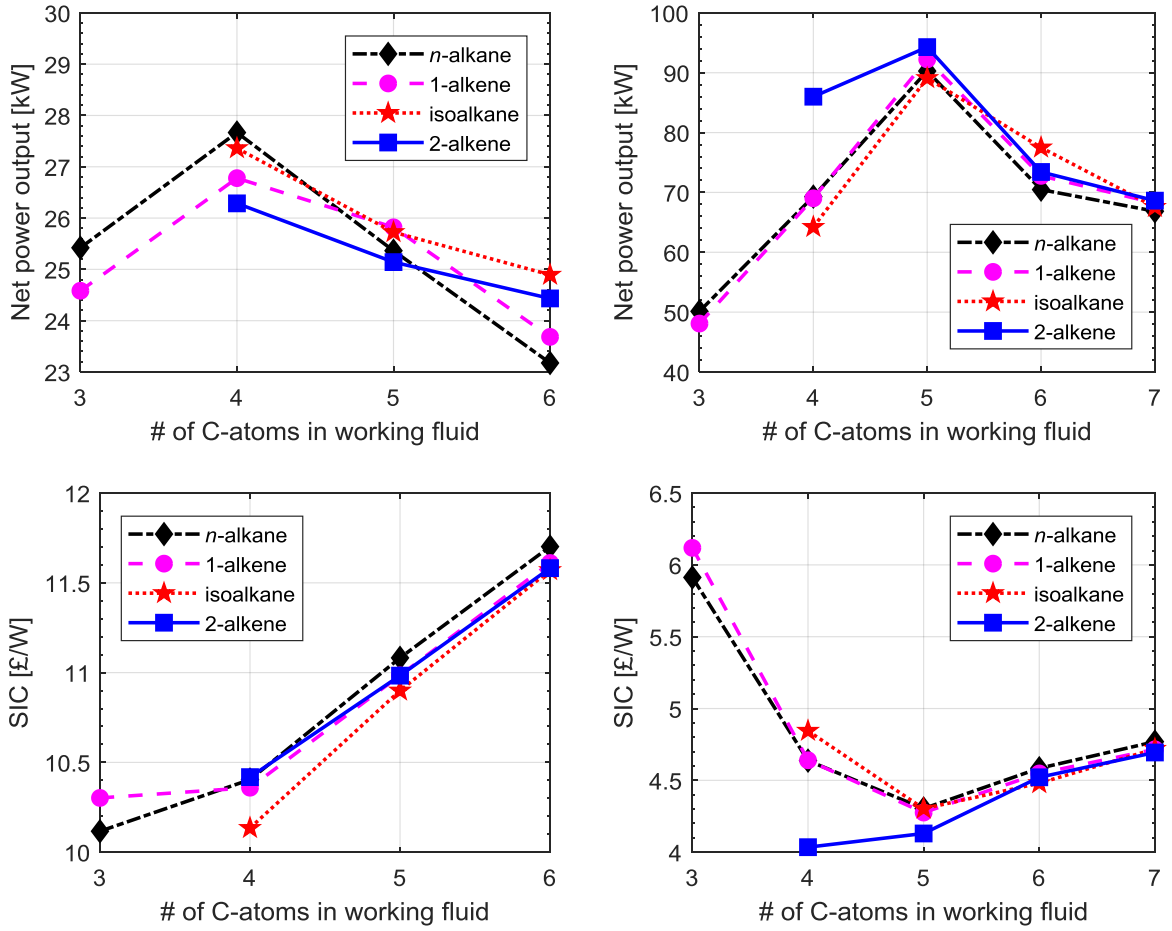

Fig. 2. (TOP) Net power output ($\dot{W}_n$) for waste-heat recovery ORC systems where SIC is optimised with different heat source temperatures $T_{h,in}$ = 150 °C (LHS) and 250 °C (RHS), respectively. (BOTTOM) Optimal specific investment costs (SIC) determined by the NLP optimisations.

In White *et al.* [2], the specific purchased equipment costs (SPEC) values corresponding to the optimised systems from Ref. [1] are determined. On average, the reported SPEC values are 49% higher than those obtained in this work, and the lowest SPEC values are achieved by iso-heptane and 2-pentene for the 150 °C and 250 °C heat sources, respectively [2]. Thus, for both the 150 °C and 250 °C case, different working fluids (propane and 2-butene respectively) are identified as having the lowest SPEC in this work. Since multiplying the SPEC with a multiplication factor results in the SIC, minimising the SIC is expected to lead to similar optimal systems to optimising the SPEC. From this comparison, it is clear that minimising the SIC indeed results in less costly systems, however, in lower capacities (net power output).

3.2. Corresponding total costs and equipment cost distribution

The total investments costs for each system are shown in Fig. 3. In the case of the 250 °C heat source, the highest TIC is required for systems with C_5 and C_6 working fluids, respectively. For a $T_{h,in}$ of 150 °C, the molecular size that achieves the highest TIC varies between the hydrocarbon families. Between the lowest and highest heat source temperature, an increase in the maximum TIC from £288,000 to £466,100 is observed. Thus, both the TIC and $\dot{W}_n$ increase with heat source

temperature. However, the highest TIC increases by a factor of roughly 1.6, whereas the highest $\dot{W}_n$ increases by a factor of 6. This illustrates how the total costs of an ORC engine increase with the capacity of the system, while the costs per kW (the SIC) decreases.

Thus, it is clear that a trade-off exists in the SIC between performance and costs. For example, if the heat source temperature is 150 °C, systems with 1-propene or propane (both C_3) as a working fluid have a lower SIC than their respective C_4 alternatives 1-butene and *n*-butane. However, systems with 1-butene and *n*-butane achieve higher $\dot{W}_n$ than those with 1-propene and propane. This is a direct illustration of how minimising the SIC represents choosing a working fluid that can achieve a high $\dot{W}_n$ at low cost. Choosing a system that maximises $\dot{W}_n$ has the potential to lead to a suboptimal SIC.

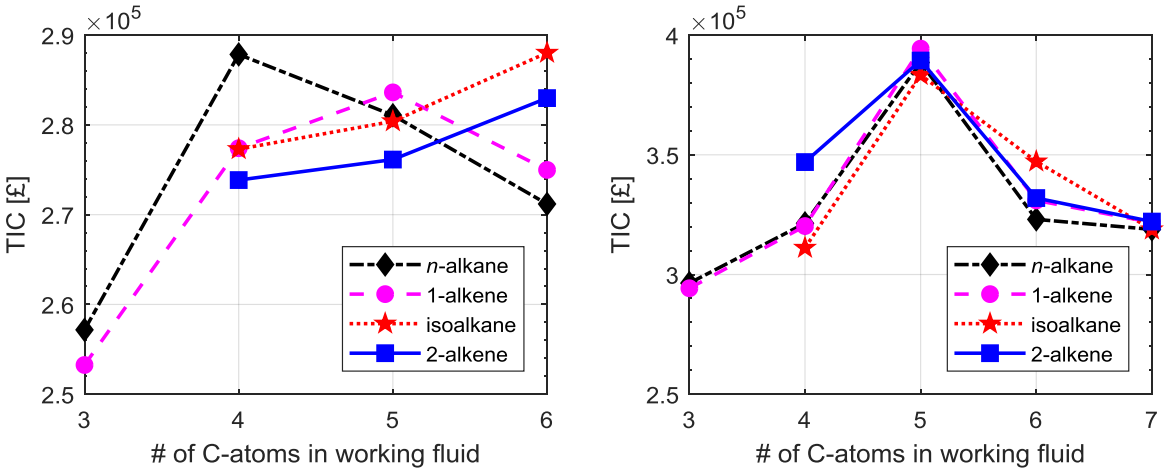

Fig. 3. Total investment costs (TIC) of waste-heat recovery ORC systems with minimum SIC with different heat source temperatures $T_{h,in}$ = 150 °C (LHS) and 250 °C (RHS), respectively.

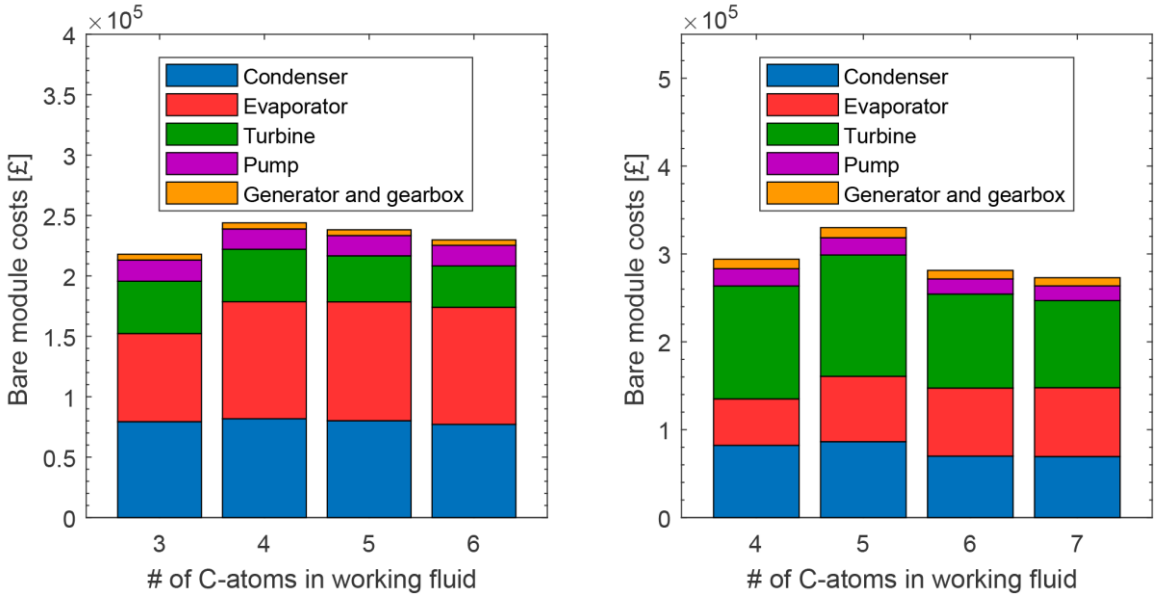

Fig. 4. Bare module costs of waste-heat recovery ORC systems for which SIC is optimised with different heat source temperatures $T_{h,in}$ = 150 °C (LHS) and 250 °C (RHS), respectively.

To compare the composition of the TIC between different working fluids and heat sources, the bare module costs are shown in Fig. 4. For each heat source, these costs are only shown for the hydrocarbon family containing the optimal working fluid. Thus, the *n*-alkanes are shown in Fig. 4 (LHS) and 2-alkenes are shown in Fig. 4 (RHS). In Fig. 3, an increase in the TIC is observed between systems with propane and *n*-butane. From Fig. 4 (LHS), it follows that this rise in the TIC can solely be attributed to an increase in the evaporator costs. Furthermore, a slight decrease in TIC

is observed between systems with *n*-butane and *n*-hexane. Between these fluids, $\dot{W}_n$ decreases, and this translates directly to a decrease in turbine costs, as can be seen in Fig. 4 (LHS).

Together the two heat exchangers account for 73.5% of total bare module costs for the 150 °C heat source, but this percentage decreases to 50.3% for the 250 °C heat source. The turbine makes up 17.1% and 40.0% of the total costs, in order of increasing $T_{h,in}$, as the costs of the turbine are directly related to the system size (*i.e.*, power generated, $\dot{W}_n$). Other general trends are an overall increase in evaporator costs and a decrease in condenser costs, when comparing the lightest and heaviest working fluids. This trend was found in results relating to both investigated heat sources.

3.3. On the choice of the objective function

In all the optimisations presented above, the objective was to minimise the SIC. To illustrate the significance of the choice of the objective function, three additional optimisations were performed for an ORC engine with 2-heptene and a higher $T_{h,in}$ of 350 °C (the lowest SIC design at this temperature). In two instances, the objective was to maximise $\dot{W}_n$, and in third instance, the objective was to minimise the TIC *(i.e.*, **f** in Eq. 11 is either min SIC, max $\dot{W}_n$ or min TIC). In one of the optimisations where $\dot{W}_n$ is maximised, minimum pinch point temperature difference constraints of 10 °C in the evaporator and condenser were applied. The results are presented in Table 4.

Table 4. Results of NLP optimisations with the objectives to minimise SIC, maximise $\dot{W}_n$ or minimise TIC. The working fluid is 2-heptene, $T_{h,in}$ = 350 °C.

Objective function	ΔT^{min} [°C]	SIC [£/kW]	$\dot{W}_n$ (kW)	TIC [£]	$T_{h,out}$ [°C]	$A_{s,ev}+A_{s,co}$ [m^2]	$\Delta T_{pinch,ev}$ [°C]	$\Delta T_{pinch,co}$ [°C]
Min. SIC	–	£2,910	150.8	£438,370	115.8	40	41.8	34
Max. $\dot{W}_n$	–	£4,560	221.2	£1,008,020	58.3	1,709	0.10	13
Max. $\dot{W}_n$	10	£4,320	210.3	£908,380	70.0	541	10.1	15
Min. TIC	–	£2,707,950	0.009	£24,475	344.2	0.00	86.1	184

The choice of objective function has a significant effect on the optimal solution. When maximising $\dot{W}_n$, the costs of the system are completely neglected. This has numerous effects on the optimal operating conditions. Since the costs of the heat exchangers are not part of the objective, low fluid velocities are identified as optimal, leading to low pressure drops to maximise performance. Furthermore, the $\Delta T_{pinch,ev}$ is only 0.1 °C. This is achieved at the inlet of the preheating section of the evaporator, and the heat source temperature shows the largest decrease for this objective. This makes intuitive sense, since this leads to the highest heat transfer rate between the heat source and the system, and therefore the possibility to generate more power. However, the small ΔT_{pinch} leads to large values for A_s. When ΔT^{min} = 10 °C, the total A_s decreases significantly. Only the temperature of the working fluid in the evaporator is limited by the pinch point constraint. Clearly, such a constraint limits $\dot{W}_n$, but also substantially reduces the required A_s and therefore the TIC. If the objective is to minimise the TIC, large values of v and ΔT_{pinch} are specified, leading to small values of A_s. As any power generation results in turbine and generator costs, $\dot{W}_n$ is effectively minimised. Finally, minimising SIC results in intermediate values for v, ΔT_{pinch}, TIC and $\dot{W}_n$.

Minimising the TIC would ultimately result in a TIC of £0 and a $\dot{W}_n$ approaching zero. However, the solver was not able to identify a set of decision variables that results in a $\dot{m}_{wf}$ of exactly zero while remaining feasible (*e.g.*, sometimes one of the A_s values would become slightly negative). Furthermore, if any equipment sizing parameter becomes zero, this results in a numerical error, since the cost correlations contain natural logarithms of these sizing parameters.

Maximising $\dot{W}_n$ requires the introduction of additional pinch point constraints that can prevent the identification of excessive A_s and TIC values. Furthermore, lower bounds on v should be specified, again to prevent excessive A_s, and the transition to different flow-regimes at which the correlations for α and ΔP_f are not applicable. Minimising the TIC requires the introduction of a minimum

requirement of $\dot{W}_n$, to prevent identification of systems with very poor performance. However, such constraints are not necessary when using the SIC as objective, and can only lead to the exclusion of solutions. From this comparison, it can be concluded that using the SIC as objective function enables the solving algorithm to make multiple trade-offs between costs and performance.

4. Conclusions

Traditionally, working fluid selection for organic Rankine cycle (ORC) engines has been via heuristics and the pre-screening of known working fluids. However, computer-aided molecular design techniques allow the selection of an optimal working fluid during ORC system optimisation. This enables the design of working fluids that fit the peculiar characteristics of the heat source and sink, and can lead to the identification of novel working fluids that would be hitherto not be found using heuristics. An existing CAMD-ORC framework developed by White *et al.* [1,2] is extended to incorporate the selection of working fluids into the optimisation procedure, while taking economic aspects into consideration when determining the optimal process design.

When the specific investment cost (SIC) is minimised, it follows that at low temperatures (*i.e.*, here at 150 °C) propane is the optimal working fluid with an SIC of £10,120/kW, while 27.7 kW of power is generated by the ORC system with *n*-butane as the working fluid. For an intermediate heat-source inlet temperature of 250 °C the best performing working fluid is 2-butene with an SIC of £4,035/kW, whereas the most power is generated by the system with 2-pentene (94.3 kW).

The result illustrates the relationship between the molecular size of the optimal working fluids and the $T_{h,in}$, with heavier and more complex fluids being optimal at higher temperatures and *vice versa*. This is brought about by their higher critical temperatures which allow evaporation to occur with relatively small temperature differences in the evaporator. Optimal operating parameters are designed to balance the trade-offs between system cost and performance. Pinch-point temperature differences in the heat exchangers are chosen by the solver to ensure non-excessive A_s requirements, but also reasonable performance. Flow velocities in the heat exchangers are chosen to represent a similar trade-off, between non-excessive A_s, and low pressure drops.

While high $\dot{W}_n$ and low SIC are related, they are not equivalent objectives and therefore do not lead to the same results. Merely maximising the $\dot{W}_n$ and/or minimising the TIC result in costly or poor performing systems. Introducing a pinch point constraint is necessary when maximising $\dot{W}_n$, to prevent the identification of systems with excessive heat exchange surface areas and costs. However, when the SIC is minimised, such pinch point constraints are not necessary as the nature of the objective requires the solver to strike a balance between the ORC system performance (which is favoured by very low pinch point constraints) and the system costs that are minimised by large temperature differences between the heat source/sink and the working fluid in the heat exchangers.

Acknowledgment

This work was supported by the UK Engineering and Physical Sciences Research Council (EPSRC) [grant number EP/P004709/1] and by the UK Department for International Development (DFID) through the Royal Society-DFID Africa Capacity Building Initiative. Data supporting this publication can be obtained on request from cep-lab@imperial.ac.uk.

References

[1] M. T. White, O. A. Oyewunmi, A. J. Haslam and C. N. Markides, "Industrial waste-heat recovery through integrated computer-aided working-fluid and ORC system optimisation using SAFT-γ Mie," Energy Conversion and Management, vol. 150, pp. 851-869, 2017.

[2] M. T. White, O. A. Oyewunmi, M. A. Chatzopoulou, A. M. Pantaleo, A. J. Haslam and C. N. Markides, "Computer-aided working-fluid design and thermoeconomic optimisation of novel ORC systems for waste-heat recovery applications," Energy, *in peer review*, 2018.

[3] C. N. Markides, "The role of pumped and waste heat technologies in a high-efficiency sustainable energy future for the UK," Applied Thermal Engineering, vol. 53(2), pp. 197-209, 2013.

[4] T. C. Hung, T. Y. Shai and S. K. Wang, "A review of organic Rankine cycles (ORCs) for the recovery of low-grade waste heat," Energy, vol. 22(7), pp. 661-667, 1997.

[5] L. Y. Ng, F. K. Chong and N. G. Chemmangattuvalappil, "Challenges and opportunities in computer-aided molecular design," Computers & Chemical Engineering, vol. 81, pp. 115-129, 2015.

[6] P. Linke, A. I. Papadopoulos and P. Seferlis, "Systematic methods for working fluid selection and the design, integration and control of organic Rankine cycles – A review," Energies, vol. 8(6), pp. 4755-4801, 2015.

[7] A. I. Papadopoulos, M. Stijepovic and P. Linke, "On the systematic design and selection of optimal working fluids for organic Rankine cycles," Applied Thermal Engineering, vol. 30(6-7), pp. 760-769, 2010.

[8] A. I. Papadopoulos, M. Stijepovic, P. Linke, P. Seferlis and S. Voutetakis, "Toward optimum working fluid mixtures for organic Rankine cycles using molecular design and sensitivity analysis," Industrial Engineering Chemical Research, vol. 52(34), pp. 12116-12133, 2013.

[9] O. Palma-Flores, A. Flores-Tlacuahuac and G. Canseco-Melchor, "Simultaneous molecular and process design for waste heat recovery," Energy, vol. 99, pp. 32-47, 2016.

[10] W. Su, L. Zhao and S. Deng, "Developing a performance evaluation model of organic Rankine cycle for working fluids based on the group contribution method," Energy Conversion and Management, vol. 132, pp. 307-315, 2017.

[11] W. Su, L. Zhao and S. Deng, "Simultaneous working fluids design and cycle optimization for organic Rankine cycle using group contribution model," Applied Energy, vol. 202, pp. 618-627, 2017.

[12] M. R. Faradonbeh, J. Abedi and T. G. Harding, "Comparative study of eight cubic equations of state for predicting thermodynamic properties of alkanes," The Canadian Journal of Chemical Engineering, vol. 91(1), pp. 101-110, 2013.

[13] V. Papaioannou, T. Lafitte, C. Avendaño, C. S. Adjiman, G. Jackson, E. A. Müller and A. Galindo, "Group contribution methodology based on the statistical associating fluid theory for heteronuclear molecules formed from Mie segments," Journal of Chemical Physics, vol. 140(5), pp. 054107, 2014.

[14] J. Gross and G. Sadowski, "Perturbed-chain SAFT: An equation of state based on a perturbation theory for chain molecules," Industrial & Engineering Chemical Research, vol. 40(4), pp. 1244-1260, 2001.

[15] T. Lafitte, A. Apostolakou, C. Avendaño, A. Galindo, C. S. Adjiman, E. A. Müller and G. Jackson, "Accurate statistical associating fluid theory for chain molecules formed from Mie segments," Journal of Chemical Physics, vol. 139(15), pp. 154504, 2013.

[16] S. Dufal, V. Papaioannou, M. Sadeqzadeh, T. Pogiatzis, A. Chremos, C. S. Adjiman, G. Jackson and A. Galindo, "Prediction of thermodynamic properties and phase behavior of fluids and mixtures with the SAFT-γ Mie group-contribution equation of state," Journal of Chemical Engineering Data, vol. 59(10), pp. 3272-3288, 2014.

[17] J. Schilling, M. Lampe, J. Gross and A. Bardow, "1-stage CoMT-CAMD: An approach for integrated design of ORC process and working fluid using PC-SAFT," Chemical Engineering Science, vol. 159, pp. 217-230, 2017.

[18] O. A. Oyewunmi and C. N. Markides, "Thermo-economic and heat transfer optimization of working-fluid mixtures in a low-temperature organic Rankine cycle system," Energies, vol. 9(6), pp. 448, 2016.

[19] O. A. Oyewunmi, A. I. Taleb, A. J. Haslam and C. N. Markides, "On the use of SAFT-VR Mie for assessing large-glide fluorocarbon working-fluid mixtures in organic Rankine cycles," Applied Energy, vol. 163, pp. 263-282, 2016.

[20] O. A. Oyewunmi, A. I. Taleb, A. J. Haslam and C. N. Markides, "An assessment of working-fluid mixtures using SAFT-VR Mie for use in organic Rankine cycle systems for waste-heat recovery," Computational Thermal Sciences: An International Journal, vol. 6(4), pp. 301-316, 2014.

[21] S. Lemmens, "Cost engineering techniques and their applicability for cost estimation of organic Rankine cycle systems," Energies, vol. 9(7), pp. 485, 2016.

[22] A. B. Jaffe, R. G. Newell and R. N. Stavins, "Economics of energy efficiency," Encyclopedia of Energy, vol. 2, pp. 79-90, 2004.

[23] J. Schilling, D. Tillmanns, M. Lampe, M. Hopp, J. Gross and A. Bardow, "From molecules to dollars: Integrating molecular design into thermo-economic process design using consistent thermodynamic modeling," Molecular Systems Design & Engineering, vol. 2, pp. 301-320, 2017.

[24] K. G. Joback and R. C. Reid, "Estimation of pure-component properties from group-contributions," Chemical Engineering Communications, vol. 57(1-6), pp. 233-243, 1987.

[25] D. Ambrose and J. Walton, "Vapour pressures up to their critical temperatures of normal alkanes and 1-alkanols," Pure and Applied Chemistry, vol. 61(8), pp. 1395-1403, 1989.

[26] S. R. S. Sastri and K. K. Rao, "A new group contribution method for predicting viscosity of organic liquids," Chemical Engineering Journal, vol. 50(1), pp. 9-25, 1992.

[27] D. Reichenberg, "New methods for the estimation of the viscosity coefficients of pure gases at moderate pressures (with particular reference to organic vapors)," AIChE Journal, vol. 21(1), pp. 181-183, 1975.

[28] S. R. S. Sastri and K. K. Rao, "A new temperature–thermal conductivity relationship for predicting saturated liquid thermal conductivity," Chemical Engineering Journal, vol. 74(3), pp. 161-169, 1999.

[29] T. H. Chung, L. L. Lee and K. E. Starling, "Applications of kinetic gas theories and multiparameter correlation for prediction of dilute gas viscosity and thermal conductivity," Industrial & Engineering Chemistry Fundamentals, vol. 23(1), pp. 8-13, 1984.

[30] T. H. Chung, M. Ajlan, L. L. Lee and K. E. Starling, "Generalized multiparameter correlation for nonpolar and polar fluid transport properties," Industrial & Engineering Chemical Research, vol. 27(4), pp. 671-679, 1988.

[31] S. R. S. Sastri and K. K. Rao, "A simple method to predict surface tension of organic liquids," The Chemical Engineering Journal and the Biochemical Engineering Journal, vol. 59(2), pp. 181-186, 1995.

[32] L. M. T. van Kleef, O. A. Oyewunmi and C. N. Markides, "Next generation high-efficiency heat recovery for power generation with advanced organic-fluid technologies," submitted, 2018.

[33] E. W. Lemmon, M. L. Huber and M. O. McLinden, NIST Standard Reference Database 23, NIST Reference Fluid Thermodynamic and Transport Properties - REFPROP. User's Guide, Version 9.1, 2013.

[34] A. R. Guy, F. Coletti and G. F. Hewitt, Heat Exchanger Design Handbook, Part 3. Begell House, 2008.

[35] J. C. Chen, "Correlation for boiling heat transfer to saturated fluids in convective flow," Industrial & Engineering Chemistry Process Design and Development, vol. 5(3), pp. 322-329, 1966.

[36] M. Dobson, J. Wattelet and J. Chato, "Optimal sizing of two-phase heat exchangers," ACRCTR-42, 1993.

[37] Z. Liu and R. H. S. Winterton, "A general correlation for saturated and subcooled flow boiling in tubes and annuli, based on a nucleate pool boiling equation," International Journal of Heat and Mass Transfer, vol. 34(11), pp. 2759-2766, 1991.

[38] M. M. Shah, "A general correlation for heat transfer during film condensation inside pipes," International Journal of Heat and Mass Transfer, vol. 22(4), pp. 547-556, 1979.

[39] M. M. Shah, "An improved and extended general correlation for heat transfer during condensation in plain tubes," HVAC&R Research, vol. 15(5), pp. 889-913, 2009.

[40] L. D. Boyko and G. N. Kruzhilin, "Heat transfer and hydraulic resistance during condensation of steam in a horizontal tube and in a bundle of tubes," International Journal of Heat and Mass Transfer, vol. 10(3), pp. 361-373, 1967.

[41] L. Friedel, "New friction pressure drop correlations for upward, horizontal and downward two-phase pipe flow." Presented at HTFS Symposium, Oxford, 1979.

[42] R. Turton, Analysis, Synthesis, and Design of Chemical Processes. (4th ed.) Upper Saddle River, N.J., 2013.

[43] W. D. Seider, J. D. Seader and D. R. Lewin, Product and Process Design Principles: Synthesis, Analysis and Design. (4th ed.) Wiley Global Education, 2008.

[44] Y. Feng and G. P. Rangaiah, "Evaluating capital cost estimation programs," Chemical Engineering, vol. 118(8), pp. 22-29, 2011.

[45] O. Odele and S. Macchietto, "Computer aided molecular design: A novel method for optimal solvent selection," Fluid Phase Equilibria, vol. 82, pp. 47-54, 1993.

[46] S. Quoilin, M. van den Broek, S. Declaye, P. Dewallef and V. Lemort, "Techno-economic survey of organic Rankine cycle (ORC) systems," Renewable and Sustainable Energy Reviews, vol. 22, pp. 168-186, 2013.